The Impact of novel Treatments on Aß Burden in Alzheimer's
Disease: Insights from a Mathematical Model

David L. Craft, Lawrence M. Wein, Dennis J. Selkoe

The Impact of Novel Treatments on Aβ Burden in Alzheimer's Disease: Insights from a Mathematical Model

David L. Craft[1], Lawrence M. Wein[2], Dennis J. Selkoe[3*]

[1] *Operations Research Center, MIT, Cambridge, MA 02139*

[2] *Sloan School of Management, MIT, Cambridge, MA 02139*

[3] *Center for Neurologic Diseases, Harvard Medical School, Brigham and Women's Hospital,*

Boston, MA 02115

---
*Person to whom correspondence should be addressed; email: selkoe@cnd.bwh.harvard.edu

Abstract

Motivated by recent therapeutic initiatives for Alzheimer's disease, we developed a mathematical model of the accumulation of amyloid β-protein ($A\beta$) in the brain. The model incorporates the production and clearance of $A\beta$ monomers, and the elongation and fragmentation of polymers by monomer aggregation and break-off, respectively. Our analysis suggests that $A\beta$ dynamics are dictated by a single unitless measure referred to as the polymerization ratio, which is the product of the production and elongation rates divided by the product of the clearance and fragmentation rates. Cerebral $A\beta$ burden attains a finite steady-state level if this ratio is less than one, and undergoes sustained growth if this ratio is greater than one. The highly nonlinear relationship between the polymerization ratio and the steady-state $A\beta$ burden implies that a modest reduction in the polymerization ratio (e.g., a 40% reduction in the production rate by a γ-secretase inhibitor) achieves a significant (e.g., 18-fold) decrease in the $A\beta$ burden. Our model also predicts that after initiation or discontinuation of treatment, it may take months to reach a new steady-state $A\beta$ burden. Taken together, our findings suggest that the research community should focus on developing agents that provide a modest reduction of the polymerization ratio while avoiding long-term toxicity. Finally, our model can be used to indirectly estimate several crucial parameters that are difficult to measure directly: the production rate, the fragmentation rate and the strength (i.e., percentage inhibition or enhancement) of treatment.

Introduction

The cerebral build-up of amyloid β-protein (Aβ) and its aggregation into oligomers and polymers are key components of the pathogenesis of Alzheimer's disease (AD) [1]. Recent studies suggest that Aβ accumulation plays an important role in AD neurodegeneration [2, 3], and a variety of Aβ treatment strategies are being aggressively pursued, including the enhancement of Aβ clearance via immunization with Aβ [1-6], and the reduction of Aβ production by inhibiting γ-secretase, which is one of the two enzymes that cuts the amyloid precursor protein (APP) to release the Aβ fragment [7, 8]. The kinetics of Aβ production, aggregation (polymerization), disaggregation and clearance, and the effect of these novel treatments on the time-dependent variation of Aβ levels are not well understood. Although there exist several mathematical models that focus on either fibrillogenesis [9-16] or plaque formation [17-19], these studies neither consider the impact of treatment nor allow for a continuously renewable source of Aβ from APP molecules. Here we formulate and analyze a simple mathematical model that tracks the dynamics of Aβ production, polymer elongation, fragmentation and clearance during the course of treatment. Simple formulas and numerical results are presented that elucidate the impact of treatment on Aβ burden.

Mathematical model

In AD brain tissue, the level of extracellular (and perhaps intracellular) Aβ (particularly Aβ_{42}, the 42 amino-acid form of Aβ) increases over time, which gives rise to polymerization. Some of these polymers cluster into light microscopically-visible particles consisting of Aβ_{42}, which can accumulate to create diffuse (amorphous) plaques, the apparent initial neuropathological lesion of AD. Further, some polymers containing Aβ_{42} and/or Aβ_{40} can eventually fold into long filamentous assemblies called amyloid fibrils, and clumped masses of these are referred to as amyloid (senile) plaques. Our mathematical model idealizes this

process in several important ways. First, we only consider extracellular $A\beta$, which is likely to be in a dynamic equilibrium with intracellular $A\beta$. We also do not distinguish between $A\beta_{40}$ and $A\beta_{42}$, or between soluble and insoluble $A\beta$, because there is insufficient information in the current literature about the precise dynamic changes in these species over time in the preclinical and clinical phases of AD. Finally, because our primary goal is to understand the impact of treatment on total cerebral $A\beta$ burden (as opposed to the number and size of plaques), we restrict our attention to $A\beta$ polymerization, and do not attempt to capture the downstream processes of fibrillization or plaque formation *in vivo*. However, later in the paper we discuss how this model might be interpreted in terms of - and generalized to incorporate plaque formation.

Our model is an infinite system of nonlinear differential equations that tracks the temporal evolution of the concentration of extracellular $A\beta$ ι-mers, for $\iota = 1, 2, \dots$. It is a variant of the Smoluchowski equation [20–21], which has been used for nearly a century to study aggregation processes such as polymerization, galaxy formation, crystallization, and cloud formation [22–23]. While this model typically considers aggregation in closed systems, the novelty of our model is to simultaneously incorporate fragmentation, a source ($A\beta$ monomer production) and a sink ($A\beta$ monomer loss).

For $\iota = 1, 2, \dots$, we let $c_i(t)$ denote the concentration of $A\beta$ ι-mer at time t; i.e., $i = 1$ denotes monomer, $i = 2$ denotes dimer, etc. The differential equations dictate the time rate of change of $c_i(t)$, denoted by $\dot{c}_i(t)$, and are given by

$$\underbrace{\dot{c}_1(t)}_{\text{monomers}} = \underbrace{p}_{\text{production}} + \underbrace{f\sum_{\iota=2}^{\infty} c_\iota(t)}_{\text{all fragmentations}} - \underbrace{c c_1(t)(2c_1(t) + \sum_{\iota=2}^{\infty} c_\iota(t))}_{\text{all elongations}} - \underbrace{l c_1(t)}_{\substack{\text{loss (e.g., by} \\ \text{degradation)}}} ,$$

(1)

4

$$\underbrace{\dot{c}_2(t)}_{\text{dimers}} = \underbrace{ec_1(t)c_1(t)}_{\substack{\text{elongation}\\\text{of monomers}}} + \underbrace{fc_3(t)}_{\substack{\text{fragmentation}\\\text{of 3-mers}}} - \underbrace{ec_1(t)c_2(t)}_{\substack{\text{elongation}\\\text{of dimers}}} - \underbrace{\frac{f}{2}c_2(t)}_{\substack{\text{fragmentation}\\\text{of dimers}}} \quad , \quad (2)$$

and for $i \geq 3$,

$$\underbrace{\dot{c}_i(t)}_{i\text{-mers}} = \underbrace{ec_1(t)c_{i-1}(t)}_{\substack{\text{elongation}\\\text{of }(i-1)\text{-mers}}} + \underbrace{fc_{i+1}(t)}_{\substack{\text{fragmentation}\\\text{of }(i+1)\text{-mers}}} - \underbrace{ec_1(t)c_i(t)}_{\substack{\text{elongation}\\\text{of }i\text{-mers}}} - \underbrace{fc_i(t)}_{\substack{\text{fragmentation}\\\text{of }i\text{-mers}}} \quad . \quad (3)$$

The model captures four processes – production, elongation, fragmentation, and loss (i.e., clearance) – and for ease of reference the corresponding mnemonic parameters are displayed in Table 1. In equation (1), Aβ monomers are produced via cleavage of the APP at a constant rate p, and are lost at time t at rate $lc_1(t)$. That is, Aβ monomers live for l^{-1} time units on average before being cleared by cell internalization (e.g., microglial ingestion), degradation by proteases or removal from the brain via the circulation.

Parameter	Description	Value
p	Production rate of Aβ monomers	1.02×10^{-11} M sec^{-1}
l	Loss rate constant for monomers	1 hr^{-1}
e	Elongation rate constant (only monomer addition)	90 M^{-1} sec^{-1}
f	Fragmentation rate constant (only monomer break-off)	3.93×10^{-6} sec^{-1}

Table 1: Some theoretical parameter values for the model, which yield a polymerization ratio of $r = pe/(fl) = 0.84$.

Equations (1)-(3) assume that elongation occurs by monomer addition with elongation constant e, so that $ec_1(t)c_{i-1}(t)$ is the rate at which $(i-1)$-mers elongate to i-mers for $i \geq 1$. Similarly, to limit the number of model parameters required, we assume that fragmentation occurs only by monomer break-offs, with fragmentation rate constant f, so the $fc_i(t)$ is the rate at which an i-mer fragments into an $(i-1)$-mer and a monomer. Hence, for $i \geq 2$, the concentrations of i-mers in equations (2)-(3) increase due to elongation of $(i-1)$-mers and fragmentation of $(i+1)$-mers, and decrease due to elongation and fragmentation of i-mers.

The factor 2 in equation (1) arises because the elongation to a dimer requires two monomers, and the term $f/2$ in equation (2) stems from the fact that a dimer can only fragment in one location, while larger i-mers possess two potential fragmentation sites. Fragmentation of dimers occurs at rate $f/2$ and creates two monomers, and hence the factors 2 and $1/2$ cancel each other out in the fc_2 term in equation (1).

An alternate modeling approach is to allow direct clearance of monomers off of i-mers (e.g., to represent microglial ingestion of polymers), rather than requiring a two-step procedure of monomer fragmentation followed by monomer clearance. This alternative would result in the omission of the "all fragmentations" term in equation (1) and the re-interpretation of f as an ingestion rate, but would not change the qualitative nature of our results: it would mainly change the precise conditions for a steady-state solution and the relative values of steady-state monomer and dimer concentrations, and slightly hasten the approach to a post-treatment steady-state. Finally, while $A\beta$ treatment parameters are not explicitly incorporated into equations (1)-(3), treatment can be included in the model, as explained later.

Results

Steady-state solution

Our analysis begins by seeking a steady-state (i.e., equilibrium) solution, c_i, to equations (1)-(3). To describe our results in a concise manner, we define the polmerization ratio

$$r = \frac{pe}{fl}, \tag{4}$$

which is a unitless quantity that incorporates the four model parameters. Setting the left side of equations (1)-(3) (i.e., the rates of change of i-mer concentration) to zero and solving for c_i reveals that there are two regimes: a steady-state (or subcritical) regime where $r < 1$

and a supercritical regime where $r > 1$. In the former case, the $A\beta$ levels settle into a steady-state where

$$c_1 = \frac{p}{l}, \quad \text{and} \quad c_i = 2\frac{p}{l}r^{i-1} \quad \text{for} \quad i \geq 2. \tag{5}$$

Hence, i−mer concentrations decay geometrically for $i \geq 2$, and monomers are more prevalent than dimers if $r < 0.5$, and less prevalent than dimers if $r > 0.5$. In contrast, if $r > 1$ then the $A\beta$ burden grows indefinitely. Because the $A\beta$ burden appears to remain relatively stable over time in symptomatic AD patients [24-26], we focus primarily on the steady-state regime, and defer until later a discussion of the supercritical regime.

Equation (5) implies that the steady-state value for the total $A\beta$ concentration (i.e., total number of $A\beta$ molecules in the system, whether they exist as monomers or i-mers), which is denoted by $c = \sum_{i=1}^{\infty} ic_i$ and referred to as the $A\beta$ burden, is given by

$$c = \frac{p}{l} \left(\frac{2}{(1-r)^2} - 1 \right). \tag{6}$$

Notice that the total $A\beta$ burden c approaches infinity as the polymerization ratio r appoaches 1. We now use equations (5)-(6) to estimate the values of the model parameters, and these parameter values, in turn, allow us to calibrate the key relationship (6) (i.e., $A\beta$ burden) to the clinical setting.

Parameter estimation

The value of the $A\beta$ monomer loss rate l in Table 1 corresponds to a half-life of 41.6 minutes, which is close to the crude experimental value of 38 minutes reported by one group in the brains of APP transgenic mice [8]. Protofibrils [27], fibrils [11, 14] and plaques [28] appear to grow primarily via $A\beta$ monomer addition, and we use an elongation rate ϵ in Table 1 taken from a synthetic fibril analysis [14], which is within a factor of two of other estimates for fibrils [11] and protofibrils [27].

The fragmentation rate f and the monomer production rate p are difficult to estimate empirically. Fortunately, we can use equations (5)-(6), together with $A\beta$ estimates from human AD brains, to estimate these two quantities as follows. A recent study [3] estimated that 1.1% of $A\beta$ in the human brain is soluble, and found that this soluble compartment consists primarily of monomers, dimers and trimers. A related study [29] measured the weighted average (of $A\beta_{40}$ and $A\beta_{42}$) soluble fraction of $A\beta$ in human brains to be 1.2%. By taking the average of these two estimates (we ignore a third estimate that is only 0.05% [30]) and assuming that the soluble dimers and trimers are exactly offset by any insoluble monomers, we equate the fraction of $A\beta$ that consists of monomers, c_1/c, to 0.013. We recognize that this analysis will underestimate the percentage of soluble $A\beta$ in the brain if there are large amounts of soluble dimers and trimers in AD brain. By equations (5)-(6), $c_1/c = (2/(1-r)^2 - 1)^{-1}$, and setting this expression equal to 0.013 yields the polymerization ratio $r = 0.84$. We also equate the $A\beta$ burden on the right side of equation (6) to the average of the total $A\beta$ levels ($A\beta_{40}$ plus $A\beta_{42}$) found in five different cortical regions of wet brain tissue of patients with a clinical dementia rating (CDR) score of 5.0 (severe dementia) in Table 1 of [2] (this estimate of 2819 pmol/g is similar in magnitude to those in [31]), by assuming that the density of wet cortical tissue (which is about 87% water) is equal to that of water. Substituting our estimates for l and r into the right side of equation (6) and equating this expression to 2819 pmol/g yields the value of the production rate p in Table 1. Finally, because $r = pe/(fl)$, the polymerization ratio estimate $r = 0.84$, together with our earlier estimates of e, l and p, yield the value for the fragmentation rate f in Table 1. Note that this value of f is about 70 times smaller than the value of the loss rate l, which suggests that within the context of our model an $A\beta$ vaccine [4, 5] that directly ingests monomers off of oligomers can be accurately represented as a fragmentation enhancer.

Aβ burden

With these parameter values in hand, we now return to equation (6) for the steady-state total Aβ burden c. This nonlinear relationship between the polymerization ratio and the steady-state Aβ burden is shown in Figure 1, and implies that a given treatment will generally achieve a greater (relative and absolute) reduction in steady-state Aβ burden for patients with higher pretreatment Aβ burdens. To position this relationship within the clinical context, we convert the Aβ burden in Figure 1 to the CDR scale using the data in Table 1 of [2]. This conversion allows us to explore the potential clinical impact (i.e., assuming that the neurodegeneration associated with Aβ can be reversed) of a reduction in the polymerization ratio via treatment. Recent studies reveal that Aβ peptide vaccination reduces not only Aβ burden but also cognitive impairment in APP transgenic mice [32, 33], implying that the neurodegeneration is at least partially reversible in mice. We note that the CDR scales on the right ordinates of Figures 1, 2 and 3 can be ignored if the reader believes that CDR will not fall in synchrony with Aβ burden in humans; the latter ordinate is still valid.

γ-secretase inhibitors

Because of their potentially adverse effect on Notch signalling [34, 37], γ-secretase inhibitors might best be used to reduce only modestly the Aβ monomer production rate, perhaps by 20-60%. To assess the effect of such treatment, we numerically solve equations (1)-(3) assuming that a symptomatic patient is in a pretreatment steady-state on days 0-250, and is administered a γ-secretase inhibitor that decreases the Aβ production rate p by 40% on days 250-620 (i.e., for 1 year). As shown in Figure 2, the post-treatment steady-state represents an 18-fold drop in the Aβ burden and a theoretical decrease in the concommitant CDR score from 5.0 (severe dementia) to 0.0 (no dementia). The perturbation dynamics in Figure 2 are rather sluggish: the relaxation time, which we define to be the time from the start of

9

treatment until the Aβ burden drops to 90% of the way towards the post-treatment steady-state (i.e., the time until the Aβ burden equals the steady-state post-treatment Aβ burden plus 0.1 times the difference of the steady-state pretreatment and post-treatment burdens) is 113 days. Interestingly, it takes much longer — about 600 days after the discontinuation of treatment — for the Aβ burden to revert to 90% of its pretreatment steady-state (assuming a polymerization ratio r of 0.84 (Table 1)).

Comparing different treatments

Equation (6) allows us to provide a comparison across various treatment approaches. Within the context of our model, treatments can affect all four parameters: γ-secretase inhibitors [7, 8], or other agents that target the upstream mechanism by which Aβ is produced from APP (e.g., β-secretase inhibitors), reduce the production rate p; agents that promote the fragmentation of monomers from polymers and/or enhance the monomer clearance rate [4, 5] increase the fragmentation rate f and loss rate l, respectively; and agents that inhibit the deposition of Aβ monomers reduce the elongation rate e. By equations (4) and (6), if the production rate p is reduced by $x\%$, then the resulting Aβ burden c is $x\%$ lower than if the elongation rate e is reduced by $x\%$. Similarly, if the fragmentation rate f is increased by $y\%$, then the resulting Aβ burden is $y\%$ higher than if the loss rate is increased by $y\%$. Hence, the parameters p and l have somewhat more leverage than e and f, respectively, in reducing the Aβ burden. Moreover, an $x\%$ reduction in the production rate (elongation rate, respectively) has the same effect as a $y\%$ increase in the loss rate (fragmentation rate, respectively), where

$$y = \frac{100x}{100 - x}. \tag{7}$$

For example, Figure 2, which was computed using a γ-secretase inhibitor that reduces the production rate by 40%, would also result from a treatment that increased the loss rate by

66.7%.

Unfortunately, there is no simple formula to compare the Aβ burden reduction achieved by changes in p vs. f or by changes in e vs. l. However, in Figure 3 we plot the post-treatment steady-state Aβ burden (and corresponding CDR score) as a function of both the percentage reduction in production rate p achieved by a γ-secretase inhibitor and the percentage increase in fragmentation rate f achieved by, e.g., an Aβ vaccine (recall that l is 70 times larger than f in Table 1). This graph strongly suggests that only a modest (e.g., 10%) change in these parameter values is required to achieve a several-fold reduction in Aβ burden and potentially a clinically significant effect on dementia. Because Aβ monomers need to be cleared after they break off, this figure also shows that an infinite fragmentation rate still leads to a finite steady-state Aβ burden, given the limits of the monomer loss rate l.

Additional computational results (not shown here) reveal that a fragmentation rate enhancer has a smaller (i.e., faster) relaxation time than a production rate inhibitor, probably because the relaxation time depends in large part on the fragmentation rate. For example, an agent that increases the fragmentation rate by 118% achieves the same post-treatment steady-state Aβ burden as the 40% γ-secretase inhibitor in Figure 2, but the relaxation time is only 40 days compared to 113 days for the γ-secretase inhibitor.

Supercritical regime

Thus far, we have assumed that $r < 1$, so that a steady-state is achieved. If $r > 1$ then the Aβ burden grows indefinitely, eventually (perhaps after many years) increasing linearly at rate $p(r-1)/r$. Moreover, for all $r \geq 1$, the distribution of polymers no longer decays geometrically, but tends over time to a uniform distribution, where each i-mer (starting with smaller values of i) successively achieves the concentration $c_1 = f/e$, $c_i = 2f/e$ for $i \geq 2$.

Hence, there are three possibilities for the effect of treatment: (i) the $A\beta$ burden is in a pretreatment steady-state and drops to a lower post-treatment steady-state, as in Figure 2; (ii) treatment causes the $A\beta$ burden to shift from the supercritical regime to the steady-state regime (Figure 4a); and (iii) treatment does not allow the $A\beta$ burden to exit the supercritical regime, although it does lower the growth rate (Figure 4b). Comparison of Figure 4a to Figure 2 shows that it may take much longer to achieve a post-treatment steady-state in case (ii) than in case (i).

Sensitivity analysis

Because we do not possess precise estimates for our parameter values, we performed a sensitivity analysis that varies the pretreatment polymerization ratio r, which is the primary driver of the $A\beta$ dynamics, according to our analysis. We use the same parameter estimation technique as before: fix l and e to their values in Table 1, find r from the fraction of $A\beta$ monomer c_1/c, use the average $A\beta$ burden of 2819 pmol/g [2] to derive p, and use r and p to calculate f. Rather than equating c_1/c to 1.3%, we now allow it to vary in order to generate a wide range of values for r, which in turn causes p and f to change. In Figures 5a and 5b, we investigate the effect caused by a 40% reduction in the production rate (via a γ-secretase inhibitor) as a function of the pretreatment polymerization ratio r. Figure 5a plots the pretreatment steady-state $A\beta$ burden divided by the post-treatment steady-state $A\beta$ burden (i.e., the fold-reduction in $A\beta$ burden), and Figure 5b shows the relaxation time, which was defined earlier. Recalling our assumption that a three-fold reduction in $A\beta$ burden leads to a clinically significant improvement in CDR score (Figure 1), Figure 5a shows that the 40% production inhibition appears capable of a significant clinical improvement for essentially all practical values of r (i.e., corresponding to percentages of monomeric $A\beta$, c_1/c, less than 30%), and a 1-to-2 log drop in $A\beta$ burden as r increases from 0.76 to 0.93. Figure 5b shows

that our base case of $r = 0.84$ is on the steep portion of the curve of relaxation time versus polymerization ratio. Hence, if the fraction of monomeric $A\beta$ is actually 5% rather than 1% of total $A\beta$, then r drops from 0.84 to 0.7 and the relaxation time decreases from 113 days to only two weeks.

Discussion

Despite the existence of some mathematical models for $A\beta$ fibrillization and plaque growth, this paper appears to represent the first attempt to use a mathematical model to assess the effect of treatment on $A\beta$ burden in Alzheimer's disease. Our model is purposefully parsimonious, and contains only four parameters: $A\beta$ monomer production rate (p), $A\beta$ monomer loss rate (l), polymer elongation rate (e), and polymer fragmentation rate (f).

The most basic result of our analysis is that there are two possible regimes, depending upon the value of the polymerization ratio r, which equals $pe/(fl)$. If this unitless quantity is less than 1, then the $A\beta$ burden enters a steady-state regime and takes on a finite value. If the polymerization ratio is greater than one, then the $A\beta$ burden grows indefinitely, eventually increasing linearly at rate $p(r-1)/r$. Researchers in other disciplines have found that the dynamics of their complex systems are dictated by a unitless measure that leads to a subcritical regime if the measure is less than 1 and a supercritical regime if the measure is greater than 1; two examples are the basic reproductive rate R_0 of an infectious pathogen in epidemiology [38] and the traffic intensity ρ in queueing theory [39]. Moreover, as with AD, in these disciplines the ultimate measures of performance (size of the epidemic and queue length, respectively) have a highly nonlinear relationship with the unitless measure. Applied researchers in these disciplines have adopted these unitless measures as a central part of their mental model of these complex systems, and routinely estimate them and monitor achieved reductions in them. We propose that AD researchers follow suit by adopting the

polymerization ratio $pe/(fl)$ as the key "Aβ driver" in this disease.

Several studies have shown that the Aβ burden does not appear to be tightly correlated with the duration or clinical severity of AD [24-26], which suggests that the polymerization ratio is less than 1 for symptomatic AD patients. Although previous mathematical models of plaque formation [18, 19] have also proposed a dynamic equilibrium of aggregation and disaggregation, the model in [19] requires that the disaggregation rate be modulated by the amount of plaque via a feedback mechanism that minimizes the changes that occur in the brain. While some feedback mechanism — for example, a cytotoxic T-lymphocyte response [40] — may exist, our model shows that when Aβ production is incorporated, a steady-state Aβ burden can be achieved by a constant fragmentation rate (i.e., in the absence of any feedback).

Nonetheless, our estimate for r is of the order of 10^{-1} (rather than 10^{-2} or smaller), and so it is conceivable that certain aggressive forms of the disease in humans or mice (strongly amyloidogenic presenilin mutations) may achieve a polymerization ratio greater than 1. More importantly, while studies [24-26] assess Aβ burden by counting plaques, a more recent study measures Aβ burden biochemically, and these more refined data suggest that Aβ burden is correlated with clinical severity of AD, which is not inconsistent with linear growth of Aβ burden (i.e., the supercritical regime in our model). Although further research may be required to further elucidate whether Aβ burden is in a steady-state or is experiencing continual growth in symptomatic AD patients, our identification of two regimes (steady-state and supercritical) suggests that there are three types of possible treatment outcomes: a reduction in Aβ burden from a pretreatment steady-state to a post-treatment steady-state (Figure 1), a change in regime from pretreatment growth to post-treatment steady-state (Figure 4a), and a reduction in growth rate from a pretreatment supercritical regime to a post-treatment supercritical regime (Figure 4b). These results suggest that the failure of a

drug to reduce the $A\beta$ burden in a subset of mice or humans may not necessarily be due to drug inactivity, but rather could signal a pretreatment supercritical regime. Also, even if the pretreatment polymerization ratio is less than 1, a patient may revert to his pretreatment $A\beta$ burden within several months after treatment is discontinued (see Figure 5b); consequently, it is important to attempt to measure the $A\beta$ burden throughout the course of treatment in a clinical trial. In contrast, if the pretreatment polymerization ratio is greater than 1, then after discontinuation of treatment a patient's $A\beta$ burden will always be smaller than if he had not received treatment.

Equation (6) provides a simple formula for the steady-state $A\beta$ burden in terms of the polymerization ratio r (provided $r < 1$) and the production rate-to-loss rate ratio, p/l. As pictured in Figure 1, the $A\beta$ burden is a highly nonlinear (increasing, convex) function of the polymerization ratio, and approaches infinity as r approaches 1. Hence, the impact of a modest reduction in r appears to be sufficient to produce a many-fold reduction in the $A\beta$ burden; for the parameter values in Table 1, a 40% reduction in the production rate via a γ-secretase inhibitor achieves an 18-fold reduction in $A\beta$ burden. Such a reduction is consistent with recently reported data in mice [5, 8] and appears to be sufficient to convert the disease process to a non-pathological state [2, 3, 29], assuming neuronal dysfunction is concommitantly decreased. Figure 1 also shows that, while the magnitude of the $A\beta$ burden reduction increases with the strength of treatment, there are decreasing returns to scale as the treatment gets stronger. Finally, our analysis predicts that the percentage reduction in $A\beta$ burden achieved by a given treatment is a unimodal function (i.e., first increasing, then decreasing) of the polymerization ratio r. For $r < 1$, the percentage reduction in $A\beta$ burden increases with r, and hence one might expect that a larger percentage reduction would be achieved in forms of AD that are particularly aggressive (e.g., the Swedish familial AD mutation [41], the trisomy 21 mutation that occurs in Down's syndrome [42]). However,

as explained in the previous paragraph, the $A\beta$ burden continues to grow in the face of treatment if the post-treatment polymerization ratio is greater than 1.

Our model is flexible enough to incorporate a variety of treatment approaches that affect any of the four model parameters. Equation (5) allows us to perform an apples-to-apples comparison of production inhibitors, elongation inhibitors, clearance enhancers, and fragmentation enhancers. For a given percentage change in parameters caused by a treatment, this analysis shows that the production inhibitors (clearance enhancers, respectively) are somewhat more effective in reducing the $A\beta$ burden than elongation inhibitors (fragmentation enhancers, respectively). Equation (7) and Figure 3 provide an explicit comparison between production inhibitors and fragmentation enhancers, and computational results show that a fragmentation enhancer attains its post-treatment steady state faster than a production inhibitor. These comparisons, coupled with future data on drug toxicity, may be useful in determining the optimal mix and level of treatments that minimize the $A\beta$ burden subject to toxicity constraints.

Figure 2 shows that it takes several months for treatment to reduce the $A\beta$ burden to a new post-treatment steady-state, and the return to a pretreatment steady-state $A\beta$ burden following the discontinuation of treatment is even more gradual. However, Figure 5b shows that the rate of $A\beta$ turnover is highly sensitive to the pretreatment polymerization ratio r, suggesting that aggressive forms of AD (having high r) are likely to take much longer to get under control. Hence, our lack of a precise estimate for the pretreatment polymerization ratio prevents us from accurately predicting the rapidity of response to treatment, but in some cases this response may be considerably quicker than suggested in Figure 2.

This general state of affairs is similar to HIV infection, as revealed several years ago in two seminal papers [43, 44]. The stability of plasma HIV levels over many years lulled the research community into believing that HIV was a relatively static disease process.

16

but a perturbation of this steady-state by a powerful protease inhibitor revealed a highly dynamic equilibrium, where a high virus production rate was offset by an equally high virus clearance rate. Hence, antiviral therapy led to a precipitous drop in plasma HIV levels, and discontinuation of treatment allowed for a rapid return of HIV levels to the pretreatment steady-state. To borrow the analogy often used in the HIV field, the water level (i.e., the $A\beta$ level) in the bath may change very slowly, but the tap (production of $A\beta$ monomer from APP) and drain ($A\beta$ loss) may be operating at deceptively high rates. It is worthwhile for AD researchers to keep in mind the lessons learned by the HIV clinical research community: (i) if toxicities of various types of agents are non-overlapping, then drug combinations (e.g., a γ-secretase inhibitor plus an $A\beta$ vaccine) are likely to outperform monotherapy; (ii) watch out for drug resistance, which is the Achilles heel of HIV treatment [15]; and (iii) given the dynamic equilibrium of $A\beta$ - which implies that AD patients may require chronic treatment and the interaction between $A\beta$ production and Notch signalling [34-37], efforts should focus on developing drugs that avoid long-term toxicity, which is beginning to plague the HIV community [16].

Several of the model parameters, particularly the production rate and the fragmentation rate, are difficult to measure *in vivo*. One benefit of our analysis is that equations (5) and (6) allow an indirect estimation of the production rate p and the fragmentation rate f given published data on the $A\beta$ burden [2] and the fraction of $A\beta$ that is monomer [3, 29] (or, more generally, any quantity, such as mean polymer length, that can be derived from the steady-state distribution of i-mers). Equation (5) can also be used to measure the strength (i.e., percentage inhibition or enhancement) of a treatment *in vivo*, given data on the pre-treatment and post-treatment steady-state $A\beta$ burdens. Moreover, a transient analysis of our model (not provided here) would allow for indirect estimation of a third model parameter from serial measurements of post-treatment $A\beta$ burden.

Our study has two important limitations. First, our model does not currently differ-entiate between the various forms of $A\beta$ ($A\beta_{40}$ vs. $A\beta_{42}$, soluble vs. insoluble). However, while we have been careful to restrict the model to $A\beta$ polymerization *per se* and ignore protofibril-to-fibril conversion and plaque growth, it is clear that our model can, in fact, be viewed as a representation of plaque growth if deposition onto plaques and fragmentation of plaques are primarily due to monomer addition and break-off, respectively. While monomer deposition onto plaques is believed to be the main form of aggregation *in vitro* [28, 47], it is quite likely that polymers coalesce *in vivo* [19]. Similarly, fragmentation of oligomers [48] and plaques may be more complex than the monomer release that is assumed here. Hence, a more realistic model of plaque growth might use a variation of Smoluchowski's equation that allows i-mers and j-mers to coalesce (e.g., at a rate proportional to $i^k j^k c_i(t)c_j(t)$, where $k = 2/3$ or 1, depending on the porosity of plaques) and allows fragmentation of monomers from the plaque surface (at rate $f i^{2/3} c_i(t)$) or the entire plaque (at rate $f i c_i(t)$). While such a model would drastically change the distribution of $A\beta$ i-mers relative to the current model (skewing the distribution towards huge polymers that represent plaques), it is unlikely to significantly alter the basic nature of our results pertaining to the $A\beta$ burden. However, to the extent that the model parameters — including the effect of treatment — vary for $A\beta_{40}$ vs. $A\beta_{42}$ or soluble vs. insoluble $A\beta$, then these model generalizations would be worth pursuing in the future.

The second main weakness of our study is that our parameter values are not necessarily indicative of human AD brains: the loss rate l was derived from the brains of mice [8], and the elongation rate c was measured from synthetic $A\beta$ in a low pH environment [11, 14]. Also, we crudely equated the fraction of $A\beta$ that is monomer with the fraction of $A\beta$ that is soluble. Our sensitivity analysis (Figures 5a-5b) suggests that, regardless of how inaccurate our parameter estimates are, a modest (several-fold) change in a parameter value caused by

treatment will still lead to a clinically significant (i.e., at last three-fold) reduction in the steady-state Aβ burden, but that the time to achieve this post-treatment steady-state (i.e., relaxation time) is quite sensitive to our parameter values.

Despite the model's simplicity, our analysis elucidates the basic nature of the kinetics of the Aβ burden in the face of etiologic treatments, and provides a framework - and a novel metric, the polymerization ratio - within which to interpret the laboratory and clinical results that are likely to be generated during the next few years. As more progress is made on the identity of the toxic moiety [3, 30], the elucidation of the inflammatory and neurotoxicity cascade, and the parameter values and mechanisms related to Aβ polymerization and plaque growth, our hope is that models such as this one will be refined and generalized to provide some guidance about the optimal way to employ the emerging anti-Aβ drug arsenal.

Acknowledgment

References

[1] Selkoe, D. J. Translating cell biology into therapeutic advances in Alzheimer's disease. *Nature* **399 (Supp)**, A23-A31 (1999).

[2] Näslund, J., Haroutunian, V., Mohs, R., Davis, K. L., Davies, P., Greengard, P. & Buxbaum, J. D. Correlation between elevated levels of amyloid β-peptide in the brain and cognitive decline. *JAMA* **283**, 1571-1577 (2000).

[3] McLean, C. A., Cherny, R. A., Fraser, F. W., Fuller, S. J., Smith, M. J., Beyreuther, K., Bush, A. I. & Masters, C. L. Soluble pool of Aβ amyloid as a determinant of severity of neurodegeneration in Alzheimer's disease. *Ann Neurol* **46**, 860-866 (1999).

[4] Schenk, D., Barbour, R., Dunn, W., Gordon, G., Grajeda, H., Guido, T., Hu, K., Huang, J. Johnson-Wood, K., Khan, K., Kholodenko, D., Lee, M., Liao, Z., Lieberburg, I., Motter, R., Mutter, L., Soriano, F., Shopp, G., Vasquez, N., Vandevert, C., Walker, S., Wogulis, M., Yednock, T., Games, D. & Seubert, P. Immunization with amyloid-β attenuates Alzheimer-disease-like pathology in the PDAPP mouse. *Nature* **400**, 173-177 (1999).

[5] Bard, F., Cannon, C., Barbour, R., Burke, R.-L., Games, D., Grajeda, H., Guido, T., Hu, K., Huang, J., Johnson-Wood, K., Khan, K., Kholodenko, D., Lee, M., Lieberburg, I., Motter, R., Nguyen, M., Soriano, F., Vasquez, N., Weiss, K., Welch, B., Seubert, P., Schenk, D. & Yednock, T. Peripherally administered antibodies against amyloid β-peptide enter the central nervous system and reduce pathology in a mouse model of Alzheimer disease. *Nature Medicine* **6** 916-919 (2000).

[6] Weiner, H. L., Lemere, C. A., Maron, R., Spooner, E. T., Grenfell, T. J., Mori, C., Issazadeh, S., Hancock, W. W. & Selkoe, D. J. Nasal administration of amyloid-beta

peptide decreases cerebral amyloid burden in a mouse model of Alzheimer's disease. *Ann. Neurol.* **48**, 567-579 (2000).

[7] Wolfe, M. S., Xia, W., Moore, C. L., Leatherwood, D. D., Ostaszewski, B. L., Rahmati, T., Donkor, I. O. & Selkoe, D. J. Peptidomimetic probes and molecular modeling suggest Alzheimer's γ-secretase is an intramembrane-cleaving aspartyl protease. *Biochem.* **38**, 4720-4727 (1999).

[8] Felsenstein, K. M. The next generation of AD therapeutics: the future is now. *Abstracts from the 7th annual conference on Alzheimer's disease and related disorders*, Abstract 613 (2000).

[9] Naiki, H., Higuchi, K., Nakakuki, K. & Takeda, T. Kinetic analysis of amyloid fibril polymerization *in vitro*. *Laboratory Investigation* **65**, 104-110 (1991).

[10] Naiki, H. & Nakakuki, K. First-order kinetic model of Alzheimer's β-amyloid fibril extension *in vitro*. *Labaratory Investigation* **74**, 374-383 (1996).

[11] Lomakin, A., Chung, D. S., Benedek, G. B., Kirschner, D. A. & Teplow, D. B. On the nucleation and growth of amyloid β-protein fibrils: detection of nuclei and quantitation of rate constants. *Proc. Natl. Acad. Sci. USA* **93**, 1125-1129 (1996).

[12] Harper, J. D. & Lansbury, P. T. Models of amyloid seeding in Alzheimer's disease and scrapie: mechanistic truths and physiological consequences of the time-dependent solubility of amyloid proteins. *Annu. Rev. Biochem.* **66**, 385-407 (1997).

[13] Walsh, D. M., Lomakin, A., Benedek, G. B., Condron, M. M. & Teplow, D. Amyloid β-protein fibrillogenesis: detection of a protofibrillar intermediate. *Journal of Biochemistry* **272**, 22364-22372 (1997).

[14] Lomakin, A., Teplow, D. B., Kirschner, D. A. & Benedek, G. B. Kinetic theory of fibrillogenesis of amyloid β-protein *Proc. Natl. Acad. Sci. USA* **94**, 7942-7947 (1997).

[15] Naiki, H., Hasegawa, K., Yamaguchi, I., Nakamura, H., Gejyo, F. & Nakakuki, K. Apolipoprotein E and antioxidants have different mechanisms of inhibiting Alzheimer's β-amyloid fibril formulation *in vitro. Biochemistry* **37**, 17882-17889 (1998).

[16] Inouye, H. & Kirschner, D. A. Aβ fibrillogensis: kinetic parameters for fibril formation from Congo red binding. *Journal of Structural Biology* **130**, 123-129 (2000).

[17] Hyman, B. T., West, H. L., Rebeck, G. W., Buldyrev, S. V., Mantegna. R. N., Ukleja, M., Havlin, S. & Stanley. H. E. Quantitative analysis of senile plaques in Alzheimer disease: observation of log-normal size distribution and molecular epidemiology of differences associated with apolipoprotein E genotype and trisomy 21 (Down syndrome). *Proc. Natl. Acad. Sci. USA* **92**, 3586-3590 (1995).

[18] Cruz, L., Urbanc, B., Buldyrev, S. V., Christie, R., Gomez-Isla, T., Havlin, S., McNamara, M., Stanley, H. E. & Hyman, B. T. Aggregation and disaggregation of senile plaques in Alzheimer disease. *Proc. Natl. Acad. Sci. USA* **94**, 7612-7616 (1997).

[19] Urbanc, B., Cruz, L., Buldyrev S. V., Havlin, S., Stanley, H. E. & Hyman, B. T. Dynamics of plaque formation in Alzheimer's disease. *Biophysical Journal* **76**, 1330-1334 (1999).

[20] von Smoluchowski, M. Drei vorträge über diffusion, brownsche bewegung und koagulation von kolloidteilchen. *Z. Phys.* **17**, 557-585 (1916).

[21] von Smoluchowski, M. Versuch einer mathematischen theorie der koagulationskinetic kolloider lösungen. *Z. Phys.* **92**, 129-168 (1917).

[22] Family, F. & Landau, D. P. Kinetics of Aggregation and Gelation. North-Holland, Amsterdam (1984).

[23] Sonntag, H., & Strenge, K. Coagulation Kinetics and Structure Formation. Plenum, New York (1987).

[24] Hyman, B. T. Marzloff, K & Arriagada, P. V. The lack of accumulation of senile plaques or amyloid burden in Alzheimer's disease suggests a dynamic balance between amyloid deposition and resolution. *J. Neuropathol. Exp. Neurol.* **52**, 594-600 (1993).

[25] Arriagada, P. V., Growdon, J. H., Hedley-Whyte, E. T. & Hyman, B. T. Neurofibrillary tangles but not senile plaques parallel duration and severity of Alzheimer disease. *Neurology* **42**, 631-639 (1992).

[26] Berg, L., McKeel, D. W., Miller, J. P., Baty, J. & Morris, J. C. Neuropathological indexes of Alzheimer's disease in demented and nondemented persons aged 80 years and older. *Arch. Neurol.* **50** 349-358 (1993).

[27] Harper, J. D., Wong, S. S., Lieber, C. M. & Lansbury, P. T. Jr. Assembly of Aβ Amyloid protofibrils: an *in vitro* model for a possible early event in Alzheimer's disease. *Biochemistry* **38**, 8972-8980 (1999).

[28] Tseng, B. P., Esler, W. P., Clish, C. B., Stimson, E. R., Ghilardi, J. R., Vinters, H. V., Mantyh, P. W., Lee, J. P. & Maggio, J. E. Deposition of monomeric, not oligomeric, Aβ mediates growth of Alzheimer's disease amyloid plaques in human brain preparations. *Biochemistry* **38**, 10424-10431 (1999).

[29] Wang, J., Dickson, D. W., Trojanowski, J. Q. & Lee, V. M.-Y. The levels of soluble versus insoluble brain Aβ distinguish Alzheimer's disease from normal and pathologic aging. *Experimental Neurology* **158**, 328-337 (1999).

23

[30] Lue, L.-F., Kuo, Y.-M., Roher, A. E., Brachova, L., Shen, Y., Sue, L., Beach, T., Kurth, J. H., Rydel, R. E. & Rogers, J. Soluble amyloid β peptide concentration as a predictor of synaptic change in Alzheimer's disease. *Am. J. Pathol.* **155**, 853-862 (1999).

[31] Gravina, S. A., Ho, L., Eckman, C. B., Long, K. E., Otvos, L. Jr., Younkin, L. H., Suzuki, N. & Younkin, S. G. Amyloid β (Aβ) in Alzheimer's Disease Brain: biochemical and immunocytochemical analysis with antibodies specific for forms ending at Aβ40 or Aβ42(43). *Journal of Biochemistry* **270**, 7013-7016 (1995).

[32] Janus, C., Pearson, J., McLaurin, J., Mathews, P. M., Jiang, Y., Schmidt, S. D., Azhar Chishti, M., Horne, P., Heslin, D., French, J., Mount, H. T. J., Nixon, R. A., Mercken, M., Bergeron, C., Fraser, P. E., St. George-Hyslop, P. & Westaway, D. Aβ peptide immunization reduces behavioral impairment and plaques in a model of Alzheimer's disease. *Nature* **408**, 979-982 (2000).

[33] Morgan, D., Diamond, D. M., Gottschall, P. E., Ugen, K. E., Dickey, C., Hardy, J., Duff, K., Jantzen, P., DiCarlo, G., Wilcock, D., Connor, K., Hatcher, J., Hope, C., Gordon, M. & Arendash, G. W. Aβ peptide vaccination prevents memory loss in an animal model of Alzheimer's disease. *Nature* **408**, 982-985 (2000).

[34] Wolfe, M. S., Xia, W., Ostaszewski, B. L., Diehl, T. S., Kimberley, W. T., & Selkoe, D. J. Two transmembrane aspartates in presenilin-1 required for presenilin endoproteolysis and γ-secretase activity. *Nature* **398**, 513-517 (1999).

[35] De Strooper, B., Annaert, W., Cupers, P., Saftig, P., Craessaerts, K., Mumm, J. S., Schroeter, E. H., Schrijvers, V., Wolfe, M. S., Ray, W. J., Goate, A. & Kopan, R. A presinilin-1-dependent gamma-secretase-like protease mediates release of Notch intra-cellular domain. *Nature* **398**, 518-522 (1999).

[36] Struhl, G. & Greenwald, I. Presinilin is required for activity and nuclear access of Notch in Drosophila. *Nature* **398**, 522-525 (1999).

[37] Ye, Y., Lukinova, N. & Fortini, M. E. Neurogenic phenotypes and altered Notch processing in Drosophila Presinilin mutants. *Nature* **398**, 525-529 (1999).

[38] Diekmann, O., Heesterbeek, J. A. P. & Metz, J. A. J. On the definition and the computation of the basic reproductive ratio R_0 in models for infectious diseases in heterogeneous populations. *J. Math. Biol.* **28** 365-382 (1990).

[39] Kelly, F. P. Stochastic Networks and Reversibility. John Wiley and Sons, New York, NY (1979).

[40] Monsonego, A., Maron, R., Bar-Or, A., Krieger, J. I., Selkoe, D. & Weiner, H. I. The role of T cell reactivity to A-Beta amyloid peptide in the pathogenic processes associated with Alzheimer's disease. *Abstracts from the 7th annual conference on Alzheimer's disease and related disorders*, Abstract 105 (2000).

[41] Citron, M., Oltersdorf, T., Haass, C., McConlogue, L., Hung, A. Y., Seubert, P., Vigo-Pelfrey, C., Lieberburg, I. & Selkoe, D. J. Mutation of the β-amyloid precursor protein in familial Alzheimer's disease increases β-protein production. *Nature* **360**, 672-674 (1992).

[42] Lemere, C. A., Blustzjan, J. K., Yamaguchi, H., Wisniewski, T., Saido, T. C. & Selkoe, D. J. Sequence of deposition of heterogeneous amyloid β-peptides and Apo E in Down syndrome: Implications for initial events in amyloid plaque formation. *Neurobiol. Disease* **3**, 16-32 (1996).

[43] Wei X., Ghosh S. K., Taylor M. E., Johnson, V. A., Emini, E. A., Deutsch, P., Lifson, J. D., Bonhoeffer, S., Nowak, M. A., Hahn, B. H., Saag, M. S. & Shaw, G. M. Vi-

ral dynamics in human immunodeficiency virus type 1 infection. *Nature* **373**, 117-123 (1995).

[44] Ho D. D., Neumann A. U., Perelson A. S., Chen W., Leonard J. M. & Markowitz M. Rapid turnover of plasma virions and CD4 lymphocytes in HIV-1 infection. *Nature* **373**, 123-126 (1995).

[45] Condra J. H., Schleif W. A., Blahy O. M., Gabrelski, L. J., Graham, D. J., Quintero. J. C., Rhodes, A., Robbins, H. L. & Shivaprakash, M. *In vivo* emergence of HIV-1 variants resistant to multiple protease inhibitors. *Nature* **374**, 569-571 (1995).

[46] Carr, A., K. Samaras. D. J. Chisholm & Cooper. D. A. Pathogenesis of HIV-1 protease inhibitor-associated peripheral lipodystrophy, hyperlipidemia, and insulin resistance. *Lancet* **131**, 1881-1883 (1998).

[47] Esler. W. P.. Stimson, E. R., Ghilardi, J. R., Vinters, H. V., Lee, J. P., Mantyh, P. W. & Maggio, J. E. *In vitro* growth of Alzheimer's disease β-amyloid plaques displays first-order kinetics. *Biochemistry* **35**, 749-757 (1996).

[48] Cherny. R. A.. Guerette, P. A., McLean, C., Legg, J. T., Fraser. F. W.. Volitakis, I., Masters. C. L. & Bush.A. I. Oligomeric Aβ in PBS-soluble extracts of human Alzheimer brain. In *Abstracts from the 7th annual conference on Alzheimer's disease and related disorders.* Abstract 62 (2000).
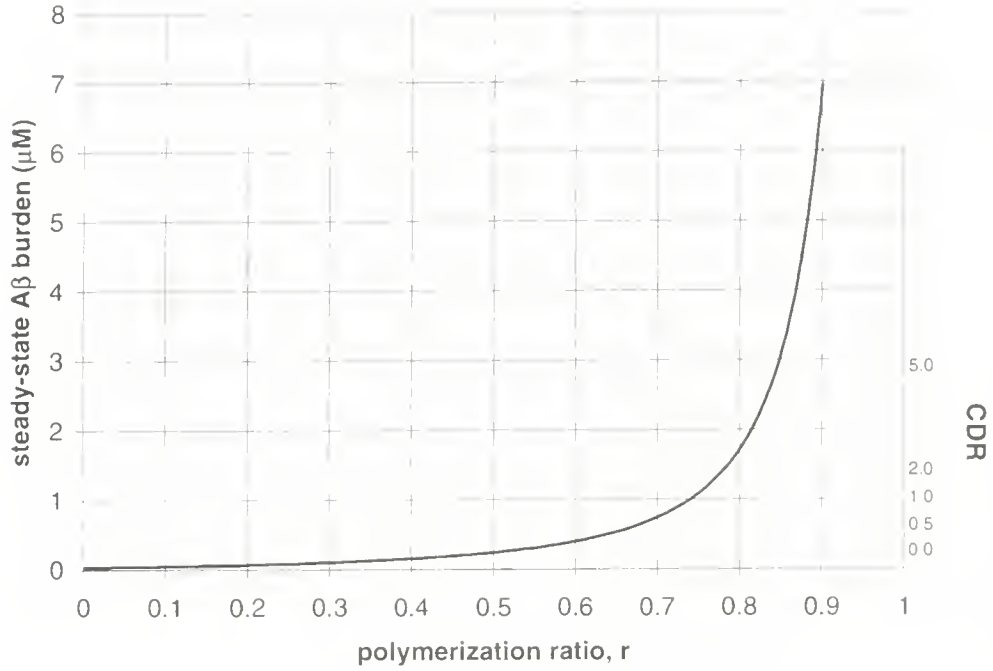
Figure 1: Steady-state Aβ burden and clinical dementia rating (CDR) score as a function of the polymerization ratio r, with p and l fixed at the values in Table 1. A CDR score of 0.0 (0.5, 1.0, 2.0 and 5.0, respectively) corresponds to no (questionable, mild, moderate, and severe, respectively) dementia. The relationship between steady-state Aβ burden (left ordinate) and CDR score (right ordinate) is based on Table 1 of [2], as explained in the text.
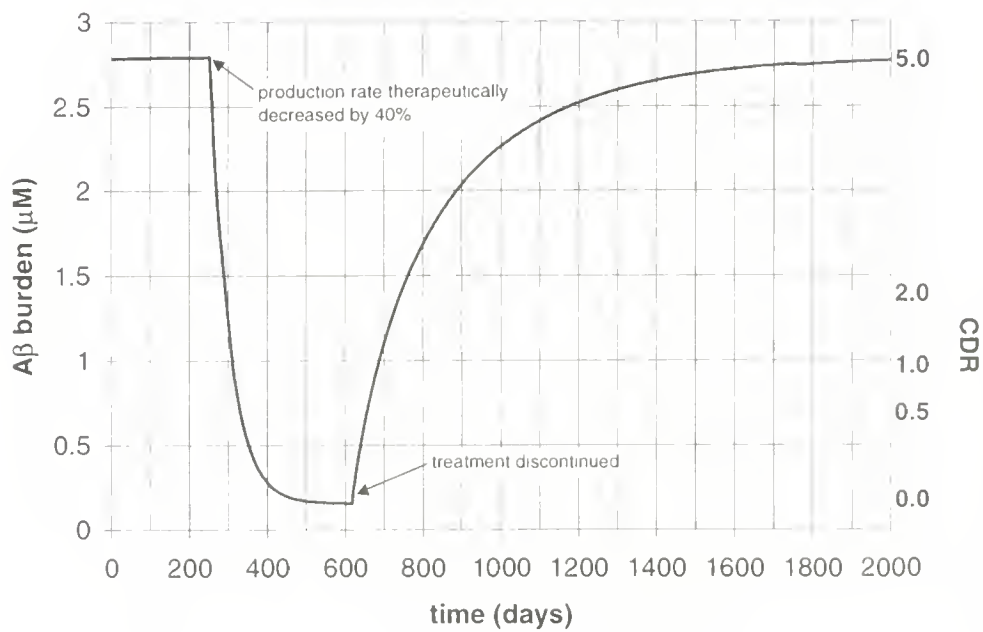
Figure 2: $A\beta$ burden and CDR score versus time. A γ-secretase inhibitor, which reduces the production rate by 40%, is administered from day 250 to day 620 (i.e., for 1 year).
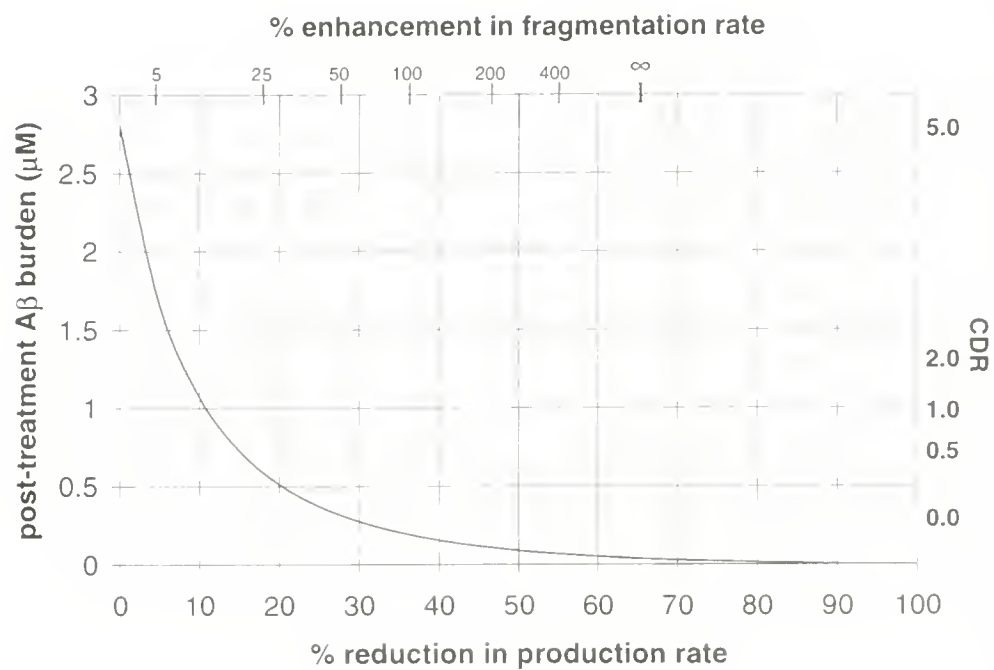
Figure 3: Post-treatment Aβ burden and CDR score versus the percentage inhibition of production rate (via a γ-secretase inhibitor) and the percentage increase in fragmentation rate (e.g., via an Aβ vaccine).
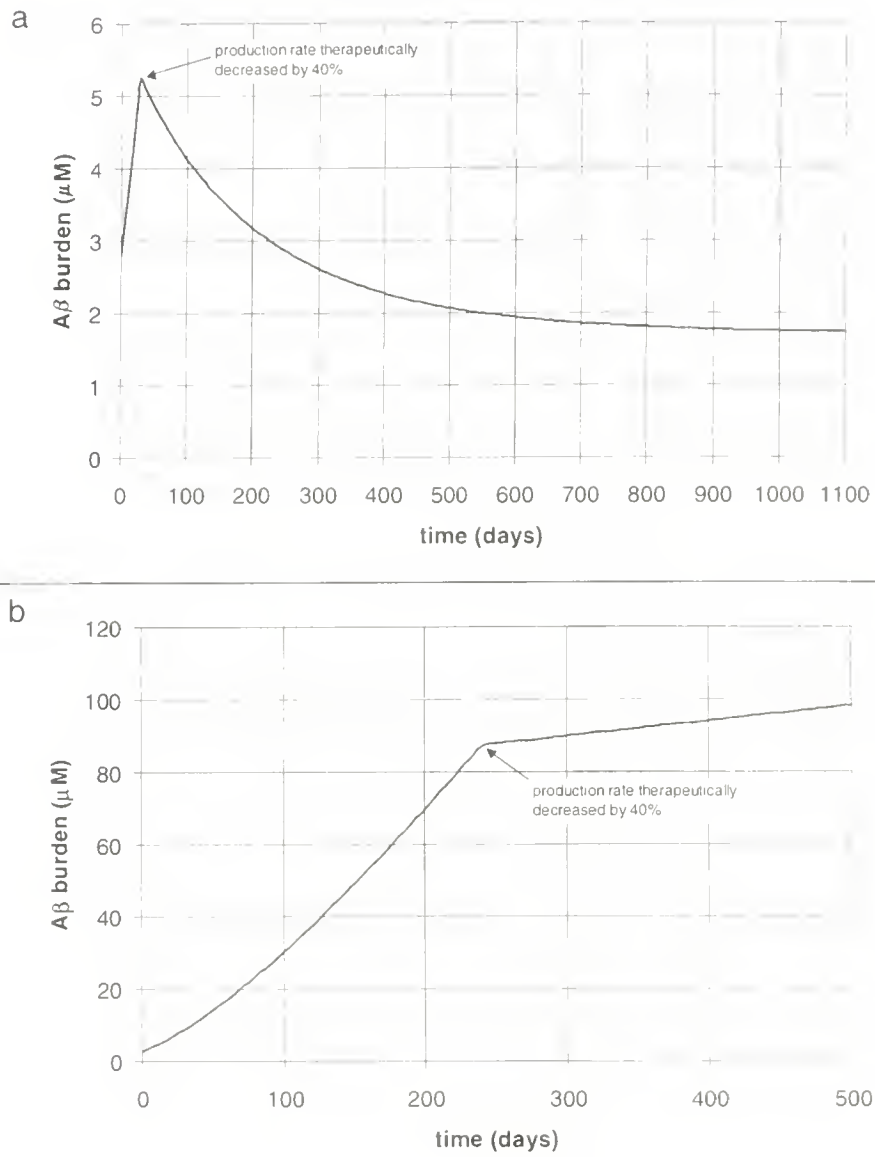
Figure 4: $A\beta$ burden and CDR score versus time. An $A\beta$ production inhibitor is begun on day 30 in (a) and on day 245 in (b), and is assumed to continue indefinitely. In (a), the polymerization ratio r is greater than 1 before treatment, and is less than 1 after treatment. In (b), the polymerization ratio r is greater than 1, both before and after the start of treatment.
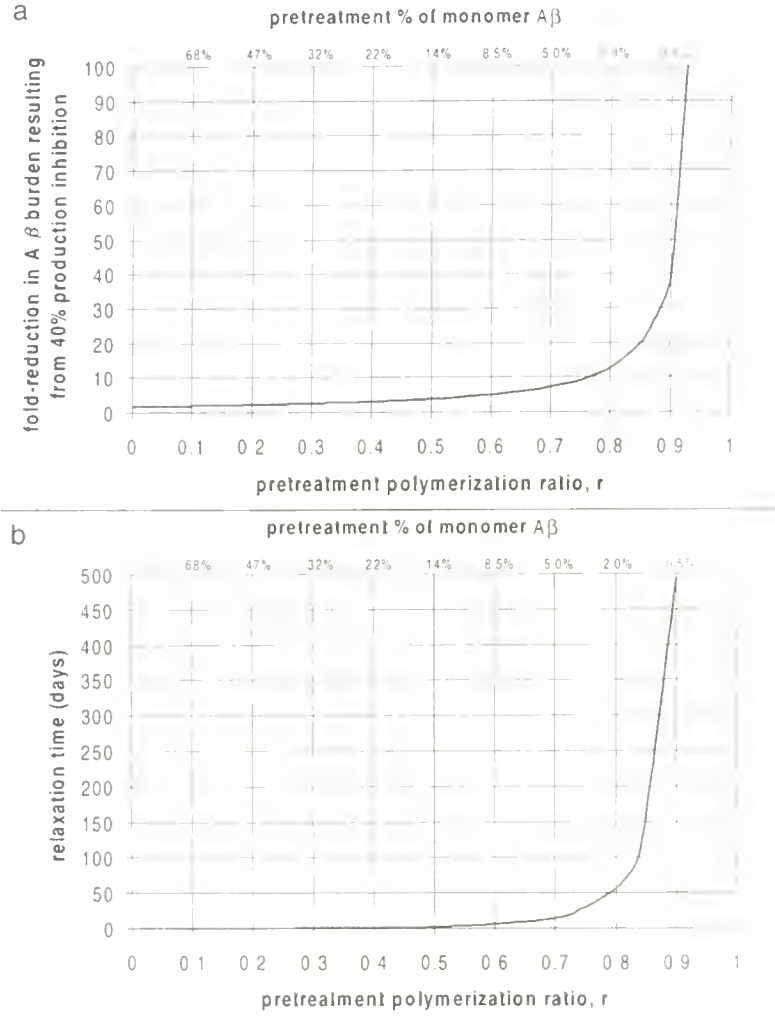
Figure 5: (a) The pretreatment steady-state $A\beta$ burden divided by the post-treatment steady-state $A\beta$ burden, as a function of the pretreatment polymerization ratio r. (b) The relaxation time (see the text for a definition) to a post-treatment steady-state $A\beta$ burden, as a function of the pretreatment polymerization ratio r. In both figures, it is assumed that a γ-secretase inhibitor reduces the production rate by 40%. In the parameter estimation procedure, r is varied by changing the fraction of $A\beta$ that is monomer (i.e., c_1/c).

31